

UCLA

UCLA Previously Published Works

Title

Communication: Chemisorption of muonium on gold nanoparticles: A sensitive new probe of surface magnetism and reactivity

Permalink

<https://escholarship.org/uc/item/7zn9n37t>

Journal

The Journal of Chemical Physics, 145(18)

ISSN

0021-9606

Authors

Dehn, MH
Arseneau, DJ
Böni, P
[et al.](#)

Publication Date

2016-11-14

DOI

10.1063/1.4967460

Copyright Information

This work is made available under the terms of a Creative Commons Attribution License, available at <https://creativecommons.org/licenses/by/4.0/>

Peer reviewed

Communication: Chemisorption of muonium on gold nanoparticles: A sensitive new probe of surface magnetism and reactivity

Cite as: J. Chem. Phys. **145**, 181102 (2016); <https://doi.org/10.1063/1.4967460>

Submitted: 25 August 2016 • Accepted: 27 October 2016 • Published Online: 11 November 2016

M. H. Dehn,  D. J. Arseneau,  P. Böni, et al.



View Online



Export Citation



CrossMark

ARTICLES YOU MAY BE INTERESTED IN

[Direct observation of muonium reacting with uncapped gold nanoparticles in porous silica and nature of the final state](#)

The Journal of Chemical Physics **152**, 184706 (2020); <https://doi.org/10.1063/5.0004210>

[Nature of magnetism in thiol-capped gold nanoparticles investigated with Muon spin rotation](#)

Applied Physics Letters **112**, 053105 (2018); <https://doi.org/10.1063/1.5017768>

[Polaronic nature of a muonium-related paramagnetic center in SrTiO₃](#)

Applied Physics Letters **115**, 192103 (2019); <https://doi.org/10.1063/1.5125919>



Time to get excited.
Lock-in Amplifiers – from DC to 8.5 GHz

[Find out more](#)

 Zurich
Instruments

Communication: Chemisorption of muonium on gold nanoparticles: A sensitive new probe of surface magnetism and reactivity

M. H. Dehn,^{1,a)} D. J. Arseneau,² P. Böni,¹ M. D. Bridges,³ T. Buck,⁴ D. L. Cortie,⁴ D. G. Fleming,⁵ J. A. Kelly,⁵ W. A. MacFarlane,⁵ M. J. MacLachlan,⁵ R. M. L. McFadden,⁵ G. D. Morris,² P.-X. Wang,⁵ J. Xiao,⁵ V. M. Zamarion,⁶ and R. F. Kiefl^{2,4}

¹Physik-Department, Technische Universität München, James-Frank-Strasse 1, 85748 Garching bei München, Germany

²TRIUMF, 4004 Wesbrook Mall, Vancouver, British Columbia V6T 2A3, Canada

³Jules Stein Eye Institute, 100 Stein Plaza UCLA, Los Angeles, California 90095, USA

⁴Department of Physics and Astronomy, University of British Columbia, 6224 Agricultural Road, Vancouver, British Columbia V6T 1Z1, Canada

⁵Department of Chemistry, University of British Columbia, 2036 Main Mall, Vancouver, British Columbia V6T 1Z1, Canada

⁶Institute of Chemistry, University of Sao Paulo, Avenida Professor Lineu Prestes 748, Sao Paulo, CEP 05508-000, Brazil

(Received 25 August 2016; accepted 27 October 2016; published online 11 November 2016)

Chemisorption of muonium onto the surface of gold nanoparticles has been observed. Muonium (μ^+e^-), a light hydrogen-like atom, reacts chemically with uncapped 7 nm gold nanoparticles embedded in mesoporous silica (SBA-15) with a strong temperature-dependent rate. The addition rate is fast enough to allow coherent spin transfer into a diamagnetic muon state on the nanoparticle surface. The muon is well established as a sensitive probe of static or slowly fluctuating magnetic fields in bulk matter. These results represent the first muon spin rotation signal on a nanoparticle surface or any metallic surface. Only weak magnetic effects are seen on the surface of these Au nanoparticles consistent with Pauli paramagnetism. *Published by AIP Publishing.* [<http://dx.doi.org/10.1063/1.4967460>]

Gold nanoparticles (GNPs) have interesting and surprising properties due to their finite size, which leads to their use in many areas,¹ e.g., medicine,² biotechnology,³ and nanotechnology.⁴ Another important application is in catalysis, especially for hydrogenation reactions.^{5–11} Although well studied, the magnetic properties of gold nanoparticles are very controversial. While bulk gold is diamagnetic, theories predict and recent studies report ordered magnetism in GNPs.¹² However, the precise nature and origin of this magnetism are unclear, and the huge discrepancy between various experimental results still lacks a conclusive explanation. A key problem in studying GNPs is that they tend to aggregate. This is often addressed by adding an organic capping layer. Magnetism is observed in thiol-capped GNPs,^{12–14} yet it is often attributed primarily to the gold sulfur bond present in such compounds instead of the finite size of the GNP. There are only a few studies investigating magnetism in uncapped GNPs,^{15–18} and with para-, ferro-, and ferrimagnetism reported, there is no consensus.

The approach chosen here is to embed uncapped GNPs in a matrix of mesoporous silica (SBA-15) and investigate magnetic properties of the surface of these nanoparticles using muon spin rotation (μ SR). Previous studies have shown that a large fraction of muons injected into fine silica powders form muonium (Mu) which escapes and thermalizes in the voids.^{19–23} Muonium (μ^+e^-) is a light hydrogen-like atom with only 1/9th the mass of hydrogen. This means that all

quantum mechanical aspects of its reactions are greatly amplified relative to its heavier cousins hydrogen and deuterium. While a great deal of information now exists on muonium reactions in the gas and liquid phase, almost nothing is known about the reactions of Mu with metal surfaces or nanoparticles.^{24,25}

In this paper, we report on Mu reacting with uncapped GNPs. We show that Mu chemisorbs on the gold and that the resulting diamagnetic or bare μ^+ state on the surface remains spin-polarized. Although the positive muon is widely known as a sensitive magnetic probe of magnetism in bulk matter or thin films, this is the first μ SR signal from a nanoparticle surface or any metallic surface for that matter. The magnetic effects we observe on uncapped 7 nm GNPs are consistent with weak rapidly fluctuating electronic moments as in a Pauli paramagnet.

A detailed description of the μ SR technique can be found elsewhere.²⁶ Basically, the time evolution of the muon spin polarization is observed directly via the parity-violating decay of the muon in which the decay positrons are emitted preferentially along the direction of the muon spin at the time of decay.

In the presence of an external magnetic field, one differentiates between transverse field (TF) geometry, where the field is applied perpendicular to the initial muon spin polarization, and longitudinal field (LF) geometry where the field direction coincides with the initial polarization. The polarization of a free muon precesses about the field direction \mathbf{B} with its Larmor frequency $\omega_\mu = \gamma_\mu |\mathbf{B}|$, where the muon gyromagnetic ratio $\gamma_\mu = 2\pi \cdot 0.013\ 55$ MHz/G. In insulators, the μ^+

^{a)}Electronic mail: mdehn@triumf.ca

may capture an electron to form Mu. The time evolution of the muon polarization for Mu is governed by both the Zeeman and muon electron hyperfine interactions. In general, the Mu TF precession signal is composed of four discrete frequencies, two of which are of the order of the hyperfine frequency $\nu_0 = 4463.3 \text{ MHz}$ ²⁷ and not observable without special detectors;^{28,29} the other two collapse for small fields, typically $\leq 10 \text{ G}$, into a single line with an effective gyromagnetic ratio $\gamma_{\text{Mu}} = 2\pi \cdot 1.39 \text{ MHz/G}$, i.e. 100 times faster than the bare muon.

Only a fraction of the incoming muons form Mu; therefore, at $t = 0$, both diamagnetic μ^+ , i.e., unbound muons precessing at or very close to the free muon Larmor frequency, and Mu are observed in silica. Those muons that stay diamagnetic and do not form Mu are called prompt. The observed asymmetry signal in a transverse magnetic field contains contributions from both components,

$$S^{\text{TF}}(t) = A_{\mu} R_{\mu}(t) \cos(\omega_{\mu} t + \phi_{\mu}) + A_{\text{Mu}} R_{\text{Mu}}(t) \cos(\omega_{\text{Mu}} t + \phi_{\text{Mu}}). \quad (1)$$

Two mesoporous silica (SBA-15) samples were investigated, one pure and one loaded with 4.5 wt. % gold nanoparticles, synthesized using a hydrothermal method.³⁰ Specific surface area measurements with the Brunauer-Emmett-Teller (BET) method³¹ yielded an area of $595 \text{ m}^2 \text{ g}^{-1}$ with a 7.5 nm average pore size for the pure silica and $431 \text{ m}^2 \text{ g}^{-1}$ surface area with a 3.9 nm average pore size for the loaded silica. The reduced pore size may be due to the chemical process of forming the GNPs. Transmission electron microscopy (TEM) gave an average nanoparticle size of $7.0 \pm 1.4 \text{ nm}$. The pinkish colour of the loaded sample was attributed to the surface plasmon resonance of the GNPs, giving clear evidence of their metallic character.

The samples were loaded into sealed titanium cells. Prior to the experiment, the cells were heated to $140 \text{ }^{\circ}\text{C}$ and pumped for 24 h to remove moisture and oxygen, and then loaded into a horizontal He gas flow cryostat while under vacuum. All measurements were taken with the LAMPF spectrometer on the M20 beamline at TRIUMF in a spin rotated mode, i.e., with the initial muon spin polarization oriented close to the vertical direction (\hat{x}) and perpendicular to the beam direction (\hat{z}).

Figs. 1(a) and 1(b) (red points) show spectra in pure SBA-15 in a TF of 6 G at two temperatures. It is evident that a large fraction of the incoming muons form Mu and, consequently, the observed signal is a composition of a diamagnetic μ^+ and Mu component. While long lived Mu is present at room temperature, there is significant damping at lower temperatures, e.g., 6 K in Fig. 1(b). The temperature dependence of the Mu relaxation rate is shown in Fig. 2 for values below 40 K, obtained by fitting Eq. (1) to the data, with $A_{\text{Mu}}, A_{\mu}, B, \phi_{\text{Mu}}, \phi_{\mu}$ unconstrained and an exponential relaxation $R_i(t) = [\exp(-\lambda_i t)]$ for both R_{Mu} and R_{μ} , where λ_{Mu} and λ_{μ} are relaxation rates for Mu and diamagnetic μ^+ . There is a gentle increase from $0.34 \text{ } \mu\text{s}^{-1}$ at $T = 289 \text{ K}$ (not shown) to $0.61 \text{ } \mu\text{s}^{-1}$ at $T = 25 \text{ K}$, below which λ_{Mu} rises sharply.

Based on previous studies on fine grained non-porous silica,²¹ we interpret the Mu relaxation in the present study of pure mesoporous SBA-15 as follows: a large fraction of

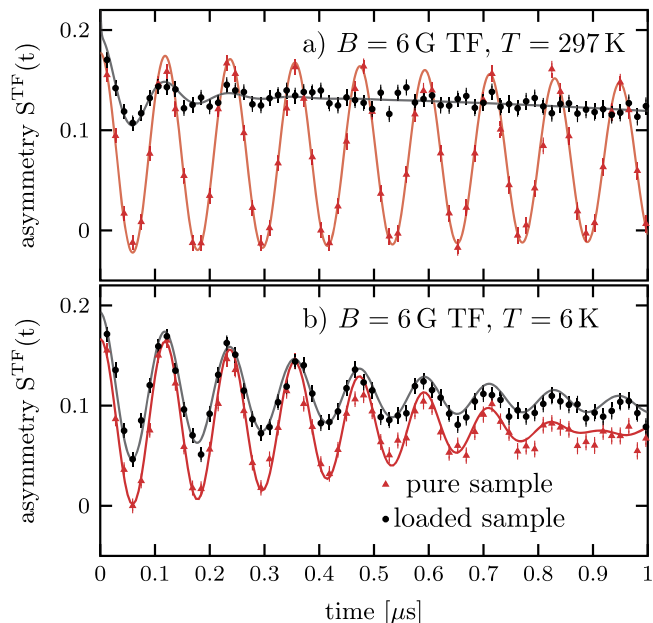


FIG. 1. Raw spectra in a transverse field of 6 G in pure (red) and gold loaded (black) SBA-15 at two temperatures. (a) $T = 297 \text{ K}$. There is long lived Mu precession in the pure mesoporous SiO_2 , while it is heavily damped in the presence of gold. (b) $T = 6 \text{ K}$. Mu relaxation rate and amplitude are comparable in both samples, indicating a similar Mu formation probability and that depolarization is dominated by the same process. Note that on the time scale of this plot, only the Mu oscillations can be observed, while the diamagnetic μ^+ component appears to be static due to its 100 times lower precession frequency.

Mu thermalizes in the porous regions of the sample on a very short time scale. At room temperature, the Mu spends most of the time off the surface and moves freely in these porous spaces. The small residual TF relaxation is attributed to both field inhomogeneity and electron spin exchange with unpaired spins from dangling bonds like $-\text{Si}-\text{O}-$ that can be produced at the high temperatures in the preparation process.³⁰ With decreasing temperature, Mu spends more time on the silica surface, as the thermal energy becomes comparable to the binding energy. At very low temperatures, Mu is bound to the surface and therefore compressed along an axis \mathbf{n} perpendicular to the surface. As a result, the hyperfine interaction is slightly anisotropic. The resulting hyperfine interaction can be decomposed into an isotropic and an anisotropic part, where the latter is characterized by the direction \mathbf{n} and magnitude ν_{ani} .²⁶ This hyperfine anisotropy (HFA) causes both the precession frequencies and their amplitudes to be dependent on \mathbf{n} , providing an explanation for the Mu TF relaxation. At base

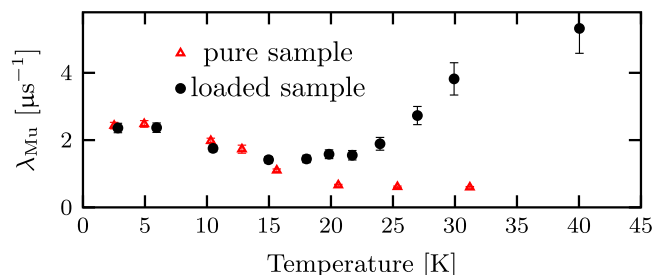


FIG. 2. Mu relaxation rate in a transverse field of 6 G, obtained in pure (red) and gold-loaded (black) SBA-15.

temperature, Mu spends essentially all its time on the surface, changing position infrequently. The signal consists of contributions from Mu with all possible values of \mathbf{n} , which causes damping. With increasing temperature, Mu changes its site more often and samples over more HFA directions during its lifetime, causing motional averaging of the HFA effects above about 25 K.

A numerical simulation based on an anisotropic Mu Hamiltonian,²⁶ an exponential distribution of surface dwell times and a random distribution of directions \mathbf{n} , yielded good qualitative agreement with both TF and LF low temperature data with an estimate of $\nu_{ani} \approx 1.5$ MHz. Details will be published elsewhere.³² The red line in Figure 1(b) represents a simulated depolarization curve for the stated ν_{ani} value.

In contrast to the pure SBA-15, the Mu TF signal in the gold-loaded SBA-15 is heavily damped at room temperature (Fig. 1(a), black points). At 6 K, however, both samples show similar spectra (Fig. 1(b)). The TF Mu relaxation rate λ_{Mu} is obtained by a fit equal to the one in the pure SBA-15. At low temperatures, λ_{Mu} agrees with the pure SBA-15 values up to 15 K, above which the fitted values increase dramatically (Fig. 2, black points).

The rapid TF Mu depolarization in the presence of the gold loaded sample is strong evidence for a chemical reaction of Mu with a GNP, resulting in a diamagnetic μ^+ on the nanoparticle's surface. At room temperature, the TF Mu precession signal in pure SBA-15 is long lived, whereas the signal is heavily damped and has a reduced amplitude in the loaded sample. At low temperatures, however, the Mu amplitude and relaxation rate in both samples are comparable, indicating a similar Mu formation probability. Thus some process involving the GNPs takes place at higher temperatures and causes damping of the Mu component. A chemical reaction of Mu with the GNPs is consistent with this: at high temperatures, the Mu is highly mobile and reaches the gold efficiently. It transforms to a diamagnetic μ^+ and stops precessing at the Mu frequency, explaining the damping. At low temperatures, the Mu is on the silica surfaces and less mobile so that it cannot reach the GNPs. Thus the TF Mu relaxation rates in both samples are dominated by HFA in this limit.

The above interpretation is further supported by the field dependence of the amplitude of the component precessing at the free muon Larmor frequency and its corresponding phase ϕ_μ . Figure 3 shows both parameters as obtained from a fit of a TF scan at $T = 297$ K to Eq. (1) with an exponential relaxation function. The phase data presented in 3(b) is corrected for instrumental field dependent shifts in the initial phase with a calibration curve obtained in the pure SBA-15, where no such change in the μ^+ amplitude was observed.

If a Mu atom reacts to form a diamagnetic μ^+ governed by an exponential reaction rate Λ much faster than the relaxation rate λ_{Mu} , the TF depolarization function $S_{Mu}^{TF}(t)$ for the muons that start out as Mu at $t = 0$ can be expressed as

$$S_{Mu}^{TF}(t) = A_{Mu} [e^{-\Lambda t} \cos(\omega_{Mu} t) + T_{Mu \rightarrow \mu}(t, B, \Lambda)], \quad (2)$$

where $T_{Mu \rightarrow \mu}(t, B, \Lambda)$ accounts for the precession signal of the reacted diamagnetic muons. Before the Mu react, their muon spin evolves with a frequency $-\gamma_{Mu} B$ with a sense of

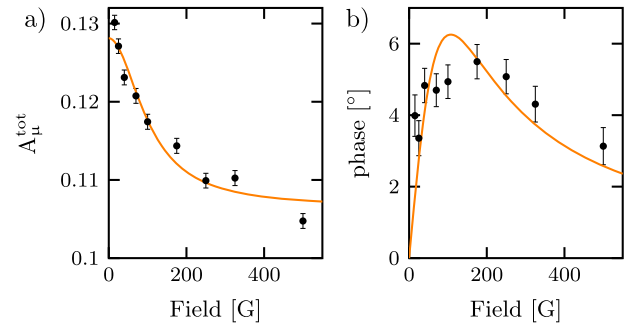


FIG. 3. (a) μ^+ amplitude A_μ^{tot} and (b) μ^+ phase as a function of applied transverse field in gold-loaded SBA-15 at $T = 297$ K. Lines represent fits to Eqs. (5) and (6), respectively.

precession opposite to that of μ^+ . Once reacted, the then diamagnetic muons precess with $\gamma_\mu B$, however with a phase shift, acquired while being Mu, compared to the prompt muons, i.e., those muons that did not form Mu at $t = 0$. For a reaction rate fast compared to the Mu precession frequency, the muon spin polarization is efficiently transferred to the diamagnetic state. $T_{Mu \rightarrow \mu}(t, B, \Lambda)$ can be expressed as

$$T_{Mu \rightarrow \mu}(t, B, \Lambda) = \int_0^\infty e^{-\Lambda t'} \Lambda \cos[\gamma_\mu B(t - t') - \gamma_{Mu} B t'] dt'. \quad (3)$$

For times $t \gg \Lambda^{-1}$, the solution of Eq. (3) simplifies to $T_{Mu \rightarrow \mu}(t \gg \Lambda^{-1}, B, \Lambda)$ and represents the time evolution of the transferred polarization in the diamagnetic state. The observed signal $S_\mu(t)$ at the muon Larmor frequency is the sum of prompt and transferred muon signal, which can be described by (compare Refs. 33 and 34)

$$S_\mu(t) = A_\mu^{\text{tot}} \cos[\gamma_\mu B t - \Phi], \quad (4)$$

with the total amplitude A_μ^{tot} , taking into account both contributions,

$$A_\mu^{\text{tot}} = \sqrt{\frac{A_{Mu}^2 + 2A_{Mu} A_\mu}{B^2(\gamma_{Mu} + \gamma_\mu)^2/\Lambda^2 + 1}} + A_\mu^2 \quad (5)$$

and a phase shift Φ

$$\Phi = \arctan \left[\frac{A_{Mu} B (\gamma_{Mu} + \gamma_\mu) / \Lambda}{A_{Mu} + A_\mu (1 + B^2 (\gamma_{Mu} + \gamma_\mu)^2 / \Lambda^2)} \right]. \quad (6)$$

The field dependence of the total μ^+ amplitude and the μ^+ phase agrees well with this model. The curves in Figs. 3(a) and 3(b) represent fits to Eqs. (5) and (6). The fit of the amplitudes yields for the prompt amplitude $A_\mu = 0.107 \pm 0.002$, the Mu amplitude $A_{Mu} = 0.022 \pm 0.002$, and the reaction rate $\Lambda = 870 \pm 181 \mu\text{s}^{-1}$; and the fit of the phase data with A_μ fixed gave $A_{Mu} = 0.026 \pm 0.003$, $\Lambda = 852 \pm 137 \mu\text{s}^{-1}$, showing good agreement with each other. Given that a Mu amplitude of $A_{Mu} \approx 0.08$ is observed at low temperatures for the loaded sample, this indicates that about 30% of the Mu reacts on a time scale fast enough to account for the drop in the total μ^+ amplitude shown in Fig. 3(a). A reaction rate of that order does not allow for any visible Mu signal, as the Mu reacts within a few nanoseconds. However, it is clear in Fig. 1(a) that such a slow component is present, suggesting that this reaction is governed by more than one time scale. That is reasonable since there is a distribution of distances between initial Mu sites and

the nearest GNP. To simplify, we suggest a fast rate Λ_f accounting for almost all coherent spin transport in TF geometry and a slow rate Λ_s . For example, if Mu emerges from the silica into a channel with a GNP, it quickly reacts, while Mu that starts out in a large void without a GNP nearby needs many collisions with the silica surface to reach a channel with gold. The time spectrum shown in 1(a) is fit accordingly to the following model (black line):

$$S(t) = A_\mu R_\mu(t) \cos(\omega_\mu t) + A_{\text{Mu}} \left[(x e^{-\Lambda_f t} + (1-x) e^{-\Lambda_s t}) \cos(\omega_{\text{Mu}} t) + (1-x) T_{\text{Mu} \rightarrow \mu}(t, B, \Lambda_s) + x T_{\text{Mu} \rightarrow \mu}(t, B, \Lambda_f) \right], \quad (7)$$

where $x = 0.3$ is the fraction of the fast component as obtained above and R_μ an exponential function. With $A_\mu = 0.107$, $A_{\text{Mu}} = 0.08$, and $\Lambda_f = 865 \mu\text{s}^{-1}$, this yields a slow reaction rate of $\Lambda_s = 12.0 \pm 1.7 \mu\text{s}^{-1}$.

Complementary information can be obtained by applying a longitudinal magnetic field (LF), i.e., along the initial polarization direction. Fig. 4(a) (red points) shows a room temperature spectrum in a longitudinal field of 10 G obtained in pure SBA-15. Again the signal is comprised of μ^+ and Mu components. All of the observed relaxation is attributed to the Mu component, which is fit to an exponential decay, consistent with spin exchange with the paramagnetic centers noted earlier. A full temperature dependence shows the Mu relaxation rate λ_{Mu} scatters around a constant value at high temperatures before it drops sharply below 30 K. This decrease at low T is consistent with relaxation from dynamic HFA. At base temperature, Mu is assumed to be static. For values of ν_{ani} of a few MHz or lower, HFA has essentially no effect on the polarization, which agrees with the near zero relaxation rate. With increasing temperature, Mu changes sites and experiences a different \mathbf{n} , causing damping. Above 30 K, the observed relaxation is most likely due to spin exchange with unpaired spins on the silica surface.

Since it is known that heat treatment of mesoporous silica can introduce paramagnetic impurities,^{30,35} one might expect a higher relaxation caused by spin-exchange in the gold-loaded sample. Yet, compared to the pure SBA-15, *less* relaxation is observed in a LF of 10 G in the loaded sample (Fig. 4(a), black points). Thus the increased damping in TF (compare Fig. 1(a))

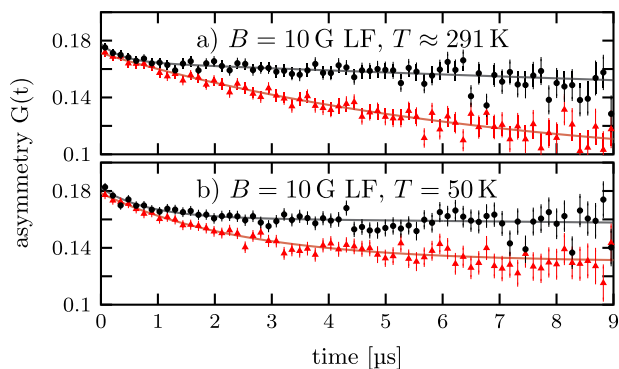


FIG. 4. Raw spectra in a LF of 10 G in pure (red) and gold-loaded (black) SBA-15 at (a) room temperature and (b) 50 K. There is less relaxation in the loaded sample, which strongly indicates a reaction to a weakly relaxing diamagnetic state on the gold surface.

is *not* due to enhanced HFA or spin exchange in the loaded sample, as both would result in more, not less, LF relaxation. On the contrary, the lower LF relaxation rate strongly supports the model of a chemical reaction: unlike in the pure SBA-15, where the highly mobile Mu is depolarized by spin exchange, it reacts on a fast time scale to form a weakly relaxing diamagnetic muon state on the gold surface. Even in the presence of the gold, there is a small fast front end, which we attribute to a small fraction of Mu spin exchanging on their way to the GNPs. Note that unlike in TF geometry, where the external field causes muon precession and therefore limits the available time window where a reaction that coherently transfers spin to the GNP can occur, no such induced depolarization happens in the presence of a longitudinal field. Consequently, the reacted muons on the gold surface have a high degree of spin polarization and act as a highly sensitive probe for any weak surface magnetism. Fig. 4(b) shows LF spectra in 10 G in both samples at 50 K. In the presence of the GNPs, little or no relaxation from the reacted muons is observed. The fit indicates that the spin relaxation on the GNP surface cannot be any bigger than about $0.05 \mu\text{s}^{-1}$. This implies any electronic moments must be fluctuating rapidly as expected from a Pauli paramagnet.

Although there are many conflicting reports of magnetism in GNPs of all different sizes, our result is reasonable considering the particles are relatively large, uncapped, and well separated. In particular the magnetism seen with other methods¹² peaks at much smaller sizes on the order of 2 nm where the Fermi wave vector ($k_F = 1.2 \text{ nm}^{-1}$) is close to the inverse diameter. Also the magnetism is strongly affected by capping¹³ and our samples have no capping. Of course on general grounds those GNPs with an odd number of atoms (valence electrons) must have at least one Bohr magneton. Thus we expect 1/2 Bohr magneton per nanoparticle on average since there is an equal amount of even and odd particles.

In conclusion, we have observed chemisorption of Mu onto the surfaces of 7 nm gold nanoparticles embedded in mesoporous SBA-15. The chemical reaction occurs on two very different time scales and leads to a final μ^+ state on the metal surface which is spin polarized. Although the positive muon is well known as a sensitive probe of magnetism in bulk matter and thin films, the current results represent the first observation of a μSR signal on a metallic NP surface or any metal surface. As such the method is sensitive to quasi static magnetic moments on surfaces which are only a few nuclear magnetons. The observed muon spin relaxation is very weak for 7 nm uncapped GNPs which is consistent with weak Pauli paramagnetism. However it should be possible to extend this work to other metal NPs where the magnetism is much stronger. For example, recent work on 13 atom Pt clusters shows a rich variety of magnetic effects that depend on the level of hydrogen loading.³⁶ Finally, Mu is widely known in quantum chemistry as a way to test first principles calculations and in particular quantum mass effects in H-atom reactivity.³⁷ The present study has established a route to extend Mu chemistry to metal surfaces. Furthermore, the observed reaction of Mu could allow the study of Mu reactions with surface adsorbed reactants on GNPs and other metallic NPs, thereby complimenting earlier work on the study of the muoniated

cyclohexadienyl radical on a fine grained silica-supported Pd catalyst.³⁸

This research was performed at the TRIUMF Centre for Materials and Molecular Science. The authors thank B. Hitti, R. Abasalti D. Vyas, and N. Thiem for excellent technical support. We would also like to thank NSERC (Canada) for financial support (Discovery grants for R.F.K., W.A.M., D.G.F., and M.J.M. and post-doctoral fellowship for J.A.K.). V.M.Z. is grateful to the Sao Paulo Research Foundation (FAPESP) for Grant No. 2014/01025-0.

- ¹M.-C. Daniel and D. Astruc, "Gold nanoparticles: Assembly, supramolecular chemistry, quantum-size-related properties, and applications toward biology, catalysis, and nanotechnology," *Chem. Rev.* **104**(1), 293–346 (2004).
- ²D. Giljohann, D. Seferos, W. Daniel, M. Massich, P. Patel, and C. Mirkin, "Gold nanoparticles for biology and medicine," *Angew. Chem., Int. Ed.* **49**(19), 3280–3294 (2010).
- ³Y.-C. Yeh, B. Creran, and V. M. Rotello, "Gold nanoparticles: Preparation, properties, and applications in bionanotechnology," *Nanoscale* **4**, 1871–1880 (2012).
- ⁴S. Eustis and M. A. El-Sayed, "Why gold nanoparticles are more precious than pretty gold: Noble metal surface plasmon resonance and its enhancement of the radiative and nonradiative properties of nanocrystals of different shapes," *Chem. Soc. Rev.* **35**, 209–217 (2006).
- ⁵G. C. Bond, P. A. Sermon, G. Webb, D. A. Buchanan, and P. B. Wells, "Hydrogenation over supported gold catalysts," *J. Chem. Soc., Chem. Commun.* **1973**, 444b–445.
- ⁶P. A. Sermon, G. C. Bond, and P. B. Wells, "Hydrogenation of alkenes over supported gold," *J. Chem. Soc., Faraday Trans. 1* **75**, 385–394 (1979).
- ⁷J. Schwank, "Catalytic gold," *Gold Bull.* **16**(4), 103–110 (1983).
- ⁸S. Lin and M. A. Vannice, "Gold dispersed on TiO₂ and SiO₂: Adsorption properties and catalytic behavior in hydrogenation reactions," *Catal. Lett.* **10**(1), 47–61 (1991).
- ⁹G. C. Bond and D. T. Thompson, "Catalysis by gold," *Catal. Rev.: Sci. Eng.* **41**(3–4), 319–388 (1999).
- ¹⁰E. Bus, J. T. Miller, and J. A. van Bokhoven, "Hydrogen chemisorption on Al₂O₃-supported gold catalysts," *J. Phys. Chem. B* **109**(30), 14581–14587 (2005).
- ¹¹C. Kartusch and J. A. Bokhoven, "Hydrogenation over gold catalysts: The interaction of gold with hydrogen," *Gold Bull.* **42**(4), 343–348 (2009).
- ¹²G. L. Nealon, B. Donnio, R. Greget, J.-P. Kappler, E. Terazzi, and J.-L. Gallani, "Magnetism in gold nanoparticles," *Nanoscale* **4**, 5244–5258 (2012).
- ¹³P. Crespo, R. Litrán, T. C. Rojas, M. Multigner, J. M. de la Fuente, J. C. Sánchez-López, M. A. García, A. Hernando, S. Penadés, and A. Fernández, "Permanent magnetism, magnetic anisotropy, and hysteresis of thiol-capped gold nanoparticles," *Phys. Rev. Lett.* **93**, 087204 (2004).
- ¹⁴M. H. Dehn and R. F. Kiefl, "Evidence for magnetism in thiol-capped gold nanoparticles observed with muon-spin-rotation" (unpublished).
- ¹⁵C.-M. Wu, C.-Y. Li, Y.-T. Kuo, C.-W. Wang, S.-Y. Wu, and W.-H. Li, "Quantum spins in Mackay icosahedral gold nanoparticles," *J. Nanopart. Res.* **12**(1), 177–185 (2009).
- ¹⁶C.-Y. Li, C.-M. Wu, S. K. Karna, C.-W. Wang, D. Hsu, C.-J. Wang, and W.-H. Li, "Intrinsic magnetic moments of gold nanoparticles," *Phys. Rev. B* **83**, 174446 (2011).
- ¹⁷W.-H. Li, S. Y. Wu, C. C. Yang, S. K. Lai, K. C. Lee, H. L. Huang, and H. D. Yang, "Thermal contraction of Au nanoparticles," *Phys. Rev. Lett.* **89**, 135504 (2002).
- ¹⁸R. Sato, S. Ishikawa, H. Sato, and T. Sato, "Magnetic order of Au nanoparticle with clean surface," *J. Magn. Magn. Mater.* **393**, 209–212 (2015).
- ¹⁹G. Marshall, J. Warren, D. Garner, G. Clark, J. Brewer, and D. Fleming, "Production of thermal muonium in the vacuum between the grains of fine silica powders," *Phys. Lett. A* **65**(4), 351–353, 1978.
- ²⁰J. H. Brewer, "Muonium in quartz," *Hyperfine Interact.* **8**(4), 375–380 (1981).
- ²¹R. F. Kiefl, J. B. Warren, C. J. Oram, G. M. Marshall, J. H. Brewer, D. R. Harshman, and C. W. Clawson, "Surface interactions of muonium in oxide powders at low temperatures," *Phys. Rev. B* **26**, 2432–2441 (1982).
- ²²D. Harshman, R. Keitel, M. Senba, R. Kiefl, E. Ansaldo, and J. Brewer, "Diffusion and trapping of muonium on silica surfaces," *Phys. Lett. A* **104**(9), 472–476 (1984).
- ²³D. R. Harshman, "Muon/muonium surface interactions," *Hyperfine Interact.* **32**(1), 847–863 (1986).
- ²⁴R. Marzke, W. Glaunsinger, D. Harshman, E. Ansaldo, R. Keitel, M. Senba, D. Noakes, D. Spencer, and J. Brewer, "MSR measurement of the reaction rate of muonium with a supported platinum catalyst," *Chem. Phys. Lett.* **120**(1), 6–10 (1985).
- ²⁵R. Marzke, D. Harshman, E. Ansaldo, R. Keitel, M. Senba, D. Noakes, and J. Brewer, "The relaxation rate of muonium as a function of temperature and loading in silica-supported platinum catalysts," *Ultramicroscopy* **20**(12), 161–167 (1986).
- ²⁶A. Yaouanc and P. D. de Rotier, *Muon Spin Rotation, Relaxation, and Resonance: Applications to Condensed Matter* (Oxford University Press, 2011).
- ²⁷D. Casperson, T. Crane, V. Hughes, P. Souder, R. Stambaugh, P. Thompson, H. Orth, G. zu Putlitz, H. Kaspar, H. Reist, and A. Denison, "A new high precision measurement of the muonium hyperfine structure interval ν_1 ," *Phys. Lett. B* **59**(4), 397–400 (1975).
- ²⁸E. Holzschuh, "Direct measurement of muonium hyperfine frequencies in Si and Ge," *Phys. Rev. B* **27**, 102–111 (1983).
- ²⁹R. F. Kiefl, E. Holzschuh, H. Keller, W. Kündig, P. F. Meier, B. D. Patterson, J. W. Schneider, K. W. Blazey, S. L. Rudaz, and A. B. Denison, "Decoupling of muonium in high transverse magnetic fields," *Phys. Rev. Lett.* **53**, 90–93 (1984).
- ³⁰H. Song, R. M. Rioux, J. D. Hoefelmeyer, R. Komor, K. Niesz, M. Grass, P. Yang, and G. A. Somorjai, "Hydrothermal growth of mesoporous SBA-15 silica in the presence of PVP-stabilized Pt nanoparticles: Synthesis, characterization, and catalytic properties," *J. Am. Chem. Soc.* **128**(9), 3027–3037 (2006).
- ³¹S. Brunauer, P. H. Emmett, and E. Teller, "Adsorption of gases in multimolecular layers," *J. Am. Chem. Soc.* **60**(2), 309–319 (1938).
- ³²M. H. Dehn and R. F. Kiefl, "Dynamics of anisotropic muonium on silica surfaces" (unpublished).
- ³³P. F. Meier, "Spin dynamics of transitions between muon states," *Phys. Rev. A* **25**, 1287–1294 (1982).
- ³⁴D. G. Fleming, D. M. Garner, L. C. Vaz, D. C. Walker, J. H. Brewer, and K. H. Crowe, *Muonium Chemistry—A Review*, Advances in Chemistry Series (American Chemical Society, 1979), Chap. 14, pp. 279–334.
- ³⁵M. Trejda, M. Ziolk, P. Decyk, and D. Duczmal, "The radical species and impurities present in mesoporous silicas as oxidation active centres," *Microporous Mesoporous Mater.* **120**(3), 214–220 (2009).
- ³⁶E. Roduner and C. Jensen, "Magnetic properties and the superatom character of 13-atom platinum nanoclusters," *Magnetochemistry* **1**(1), 28 (2015).
- ³⁷S. Mielke, B. Garrett, D. Fleming, and D. Truhlar, "Zero-point energy, tunnelling, and vibrational adiabaticity in the $\text{Mu} + \text{H}_2$ reaction," *Mol. Phys.* **113**(2), 160–175 (2015).
- ³⁸M. Schwager, H. Dilger, E. Roduner, I. D. Reid, P. W. Percival, and A. Baiker, "Surface diffusion of the cyclohexadienyl radical adsorbed on silica and on a silica supported Pd catalyst studied by means of ALC- μ SR," *Chem. Phys.* **189**(3), 697–712 (1994).